

Goniothalamine and Its Analogues as Potential Inhibitors of *Plasmodium falciparum* Lactate Dehydrogenase Enzyme: Molecular Docking, Molecular Dynamics Simulation Studies, and Pharmacokinetics Analysis

Sharinah Ideris^{1,2}, Syahrul Imran^{1,2}, Normala Abd Latip^{3,4} and
Che Puteh Osman^{1,2*}

¹Atta-ur-Rahman Institute for Natural Product Discovery, Universiti Teknologi MARA Cawangan Selangor, Kampus Puncak Alam, 42300 Bandar Puncak Alam, Selangor, Malaysia

²Faculty of Applied Sciences, Universiti Teknologi MARA, 40450 Shah Alam, Selangor, Malaysia

³Faculty of Pharmacy, Universiti Teknologi MARA Cawangan Selangor, Kampus Puncak Alam, 42300 Bandar Puncak Alam, Selangor, Malaysia

⁴Integrative Pharmacogenomics Institute (iPROMISE), Universiti Teknologi MARA Cawangan Selangor, Kampus Puncak Alam, 42300 Bandar Puncak Alam, Selangor, Malaysia

*Corresponding author (e-mail: cheputeh@uitm.edu.my)

Malaria has been a major concern worldwide due to the resistance of malarial parasites to most of the available antimalarial drugs. Therefore, developing new drugs is necessary to overcome this drug resistance. *Plasmodium falciparum* lactate dehydrogenase (*pf*LDH) is a gene necessary for the survival of plasmodium parasites and is a potential antimalarial target. Our objective was to discover goniothalamine and its twenty-nine analogues as potent antimalarial molecules with *pf*LDH inhibitory activity effective against resistant strains of plasmodium parasites. The molecular docking studies of the compounds were performed by AutoDock 4.2. The interaction of ligands and receptor bindings was visualized by Discovery Studio Visualizer 4.0. The Molecular dynamics simulation was carried out using Desmond v.2018. Pharmacokinetics Analysis of the compounds was done using Molinspiration tools and the pKCSM server. Molecular docking analysis showed that compounds 3,5-dimethoxy goniothalamine (-6.29 kcal/mol), parvistone (-6.22 kcal/mol), and 8-acetylgoniotriol (-6.19 kcal/mol) exhibited higher binding energy than existing drugs of chloroquine (-6.11 kcal/mol) against *pf*LDH protein. Further, these compounds show multiple interactions with the active sites of the *pf*LDH protein. In addition, these compounds fulfill the drug-likeness properties and pass the ADMET prediction. The results from the molecular dynamics simulations indicate that the 3,5-dimethoxy goniothalamine shows promising inhibitors towards *pf*LDH protein. The results showed that the selected compounds exhibit promising antimalarial activities, which are crucial considerations in drug design and development.

Keywords: Malaria; *Plasmodium falciparum* lactate dehydrogenase; goniothalamine; molecular docking; molecular dynamics

Received: September 2023; Accepted: November 2023

Malaria remains a significant global health issue, with an estimated 247 million cases and 619000 deaths worldwide in 2021. It was reported that 76% of malaria deaths worldwide involved children under five years. About 13.3 million pregnancies were exposed to malaria infection during pregnancy [1]. The emergence of drug-resistant strains of *Plasmodium* parasites, primarily *Plasmodium falciparum*, poses a substantial challenge to effective malaria control and elimination efforts. Artemisinin-based combination therapies (ACTs) have been instrumental in treating malaria and contributed to reducing the disease burden. However, the emergence of artemisinin-resistant *Plasmodium falciparum* in the Greater Mekong region is a cause for concern [2]. The resistance is characterized by the point mutation

in the parasite Kelch-like protein that impacts the effectiveness of artemisinin drugs and is associated with increased treatment failure rates of ACTs in Cambodia and Thailand [3]. Resistance to other anti-malarial drugs, such as chloroquine and antifolate drugs, has also emerged due to mutations in the genes encoded for dihydrofolate reductase (DHFR) and dihydropteroate synthase (DHPS) enzymes [4]. The resistant strains with point mutations in the genes encoding for the *Plasmodium falciparum* chloroquine resistance transporter (*pf*CRT) protein and *Plasmodium falciparum* multidrug resistance 1 (*pf*MDR1) have been linked to resistance in the parasites against various drugs [5]. The mutation of the cytochrome b gene is associated with resistance to atovaquone [6].

Therefore, ongoing research and development efforts are focused on identifying new antimalarial compounds that effectively target parasites while minimizing the development of drug resistance.

The lactate dehydrogenase enzyme (LDH) is a glycolytic enzyme crucial for energy production in *Plasmodium* parasites, making it essential for their survival [7]. Energy metabolism plays a vital role in the parasite's survival, particularly during its blood stages. Within the blood stages of the parasite, LDH is expressed at high levels in mature parasites [8]. Inhibition of *pf*LDH could potentially starve the parasite by reducing the production of lactate, which is a key step in the glycolytic pathway and crucial for energy generation in the malaria parasite [9]. It has been reported that chloroquine interacts specifically with the LDH enzyme in the NADH binding site [10]. Chloroquine's mechanism of action involves competing with NADH and acts as a competitive inhibitor for this glycolytic enzyme *pf*LDH. The dependence of the parasite on glycolysis for energy makes *pf*LDH considered a potential molecular drug target for developing new drugs due to a potential molecular target for developing new antimalarial drugs.

The genus *Goniothalamus* consists of 160 species found in Southeast Asia tropical forests. Some of these species have been widely used in traditional medicine [11]. Styryl lactones are a group of secondary meta-bolites reported mainly within the genus *Goniothalamus*. One of the well-known naturally occurring styryl lactones is goniothalamin **1**, first

isolated from the dried bark of *Cryptocarya caloneura* in 1967 (**Figure 1**). It has also been found in various species of *Goniothalamus* [12]. Compound **1** and its analogues represent natural and synthetic chemicals that have been demonstrated to possess an interesting variety of biological activities. Recent studies have demonstrated that compound **1** exhibits antimalarial activity, mainly through the *pf*LDH assay. The combination of compound **1** and chloroquine has been shown to enhance parasitemia reduction and extend the survival of treated mice [13]. Structure-activity relationship (SAR) studies have revealed that specific features of compound **1**'s structure, such as the Michael acceptor sub-unit in the lactone ring, the trans-oriented double bond in the linker part, and the configuration of the stereogenic center carbon, contribute to its biological activity [14].

In this study, molecular docking was used to evaluate the binding energies and interactions of goniothalamin **1** and its analogues against potential therapeutic drug targets such as *pf*LDH. The potential inhibitors were selected based on the highest binding energy and the important hydrogen bond interactions. The selected compounds were subjected to further analyses, including physicochemical characterization, bioactivity scoring, ADME, and toxicity. Finally, a selected compound was subjected to molecular dynamics simulation to study the stability of the ligand-receptor complex. The results showed that the selected compounds exhibit promising antimalarial activities, representing a significant step forward in developing effective antimalarial drugs.

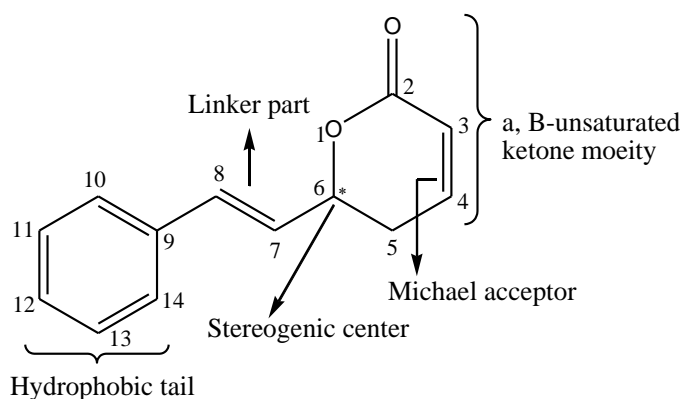


Figure 1. Sources of the activity in goniothalamin **1** structure

EXPERIMENTAL

Ligand Preparation

Goniothalamine **1** and twenty-nine (29) analogue structures were obtained from a literature review and Pub-Chem Compound database (<http://pubchem.ncbi.nlm.nih.gov/>) (**Figure 2**). The 3D structures of ligands were built in Chem3D Ultra 8.0, and energy was minimized using the MMFF94 force field.

Preparation of Protein

The X-ray crystal structure of the protein *pf*LDH (PDB ID: 1CET) [10] was obtained from Protein Data Bank (www.rcsb.org). This structure has been chosen because it has chloroquine bound to the enzyme's

active site [15]. Protein files (PDB) were further optimized by removing the bound ligands and water molecules. Hydrogen atoms and Kollman charges were added to the proteins during protein preparation.

Molecular Docking

Molecular docking studies were carried out using AutoDock 4.2. Configuration files were created for the proteins by setting suitable Cartesian coordinates to generate the Grid box. The active grid was generated for docking with 40 x 40 x 40 along with x, y, and z coordinates, 36.211, 10.539, and 19.830, respectively, with 0.375 Å grid spacing. The docking study was performed using the Lamarckian-Genetic Algorithm (LGA) method with default parameters, and the docking runs were set at 150 conformations per ligand.

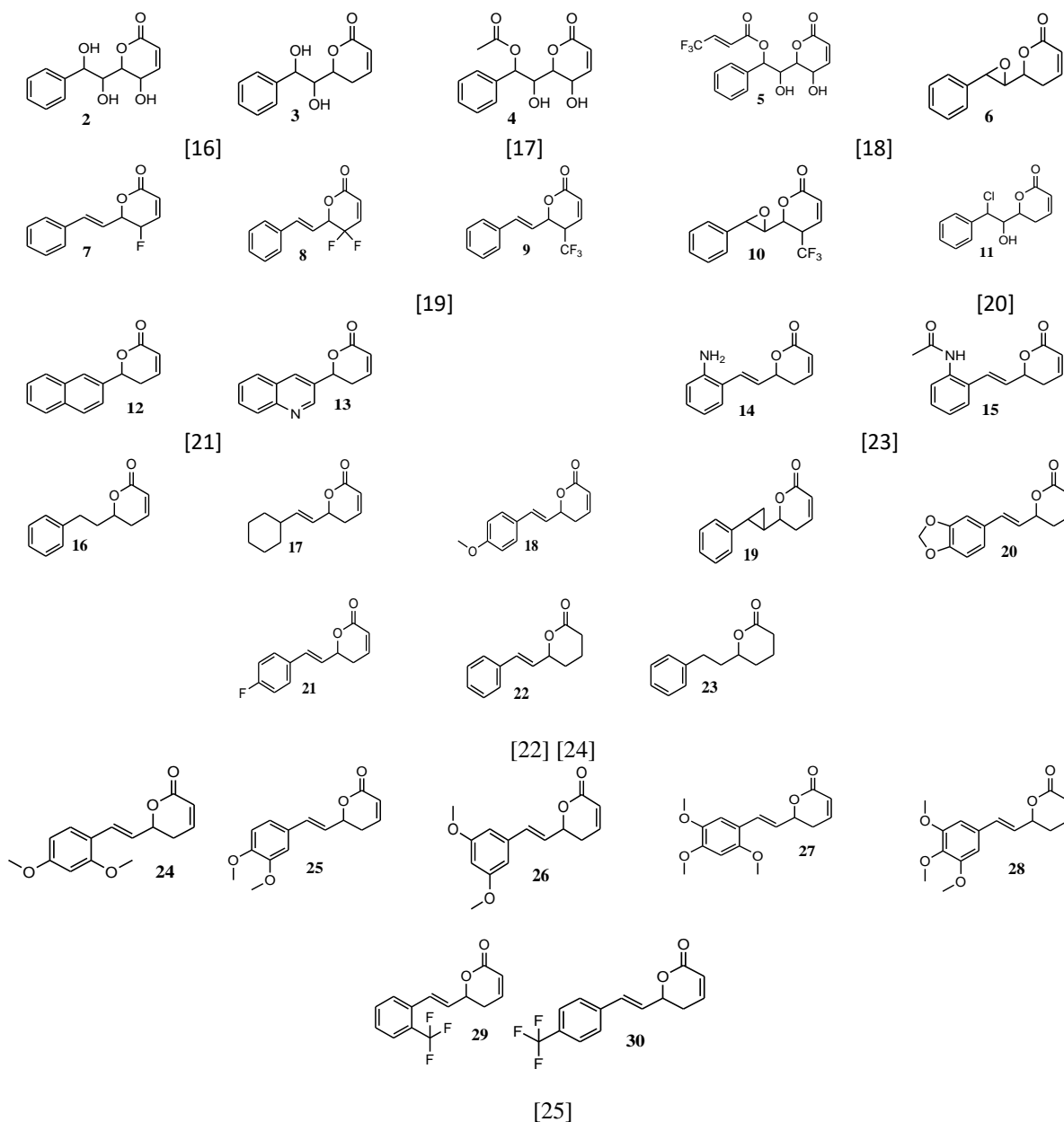


Figure 2. Chemical structures of ligands used in molecular docking studies.

Toxicity Prediction

Osiris Property Explorer calculator was used to predict the toxicity profile of compounds (<https://www.organic-chemistry.org/prog/peo/>). The toxicity results of each compound were calculated and compared with the chloroquine and pyrimethamine.

Physicochemical Properties and Bioactivity Score

The physicochemical properties and bioactivity score of the compounds were predicted with the Molinspiration molecular properties calculator (<https://www.molinspiration.com/>). Molinspiration was applied to predict the molecular properties of the compounds such as logP, polar surface area, number of hydrogen bond donors and acceptors, and others, as well as prediction of bioactivity score for the most important drug targets like G-protein coupled receptors ligand (GPCR), ion channel modulator, a kinase inhibitor, and nuclear receptor ligand [26, 27].

ADME Studies

The selected compounds' ADME (absorption, distribution, metabolism, and excretion) profiles were examined to determine their activity within the human body. The ADME characteristics of the ligands were assessed using pkCSM [28] and SWISSADME [29]. The ligand's structure SMILE was retrieved from the Pub-Chem compound database and used as the pkCSM and SWISSADME online tool input file.

Molecular Dynamics Simulation Study

In this study, the stability of the 3,5-dimethoxy goniothalamine **26** *pf*LDH complex was analyzed through Molecular Dynamics (MD) simulation for 100 ns. MD simulation of the selected protein-ligand complex **26** was carried out using Desmond v.2018. The simulation system was solvated with TIP3P water molecule in an orthorhombic box at a minimized volume of 10 Å distance and was assigned with the OPLS3 force field.

Complex **26** with target protein was assigned with enhanced Optimized Potentials for Liquid Simulations (OPLS3e) molecular mechanics force field before being subjected through minimization. The complex was then placed in an orthorhombic box with minimized volume at a distance of 10 Å and solvated using the transferable intermolecular potential 3P (TIP3P) water model. The system was further minimized with 2000 steps of conjugate gradient minimization. The system was set to 2.0 fs, 9 Å, 300K, and 1.01325 bar for the cut-off radius for time step, van der Waals, initial temperature, and pressure, respectively. The system was then heated from 0 to 300 K for 1 ns in the NVT ensemble. Finally, MD simulations were performed under the NPT ensemble for 100 ns. The result was recorded for every 50 ps with a total of 2000 frames.

RESULTS AND DISCUSSION

Validation Docking

A validation docking simulation was performed using the native ligand chloroquine and the protein structure of 1CET. This was done to ensure the accuracy and reliability of the docking method for this specific protein-ligand interaction. The binding pocket of the *pf*LDH enzyme with chloroquine was defined to include specific amino acid residues of Ala98, Glu122, Ile54, Ile119, Phe52, and Val26. These residues collectively create a binding groove near the enzyme's surface, where the ligand chloroquine is known to interact [30]. The Root Mean Square Deviation (RMSD) value obtained from re-docking the native ligand chloroquine against 1CET (**Figure 3**) was 1.80 Å. Since the value is less than the specified threshold of 2.0 Å, it suggests the acceptable accuracy of the docking method. For validation of the docking method, if the RMSD is below the threshold (2.0 Å), it indicates that the method is reliable in reproducing known binding poses [31, 32]. Potential inhibitors in this study were selected based on the binding energy scoring calculated by AutoDock 4.2 and were analyzed for important hydrogen bond interactions.

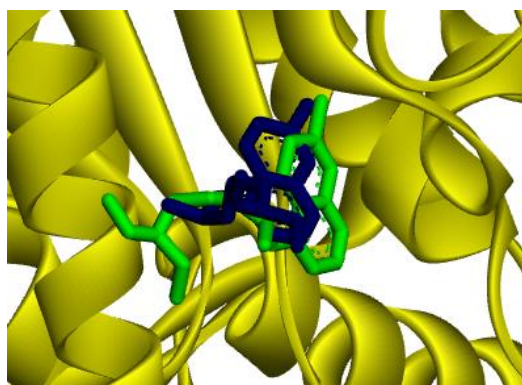


Figure 3. Validation of the docking protocol: the blue color represents the native ligand and the green color is the docked ligand.

Molecular Docking Analysis

The docking result showed that compounds **15** (-6.74 kcal/mol), **12** (-6.33 kcal/mol), **26** (-6.29 kcal/mol), **11** (-6.22 kcal/mol), **4** (-6.19 kcal/mol), and **28** (-6.15 kcal/mol) had demonstrated higher binding energies when docking with the *pf*LDH protein compared to the reference antimalarial drugs, chloroquine (-6.11 kcal/mol) and pyrimethamine (-5.88 kcal/mol) (**Table 1**). This suggests that these compounds might be effective inhibitors by binding tightly to the target protein and interfering with its function.

Table 1 indicates various interactions between the protein and thirty compounds binding and reference drugs, especially conventional hydrogen bonding interaction. Amino acids responsible for the binding of chloroquine in the *pf*LDH binding site are Ala98, Glu122, Ile54, Ile119, Phe52, and Val26. These amino acids play a crucial role in the binding of ligands to the protein [30]. Compounds **4**, **11**, **12**, **15**, **26**, and **28** also make specific interactions in the *pf*LDH binding site. Notably, the binding interactions formed involved most of the compounds with *pf*LDH protein, which are important amino acids responsible for the chloroquine interaction [33]. Compounds **12**, **15**, and **28** do not form conventional hydrogen bonds with important amino acids responsible for the chloroquine interaction. Compounds **4**, **11** and **26** have been chosen for further analysis due to their strong interactions with important amino acids, especially through conventional hydrogen bonds with Glu122 and Ile54.

Figure 4 illustrates the 2D and 3D-binding sites between the selected compounds (**4**, **11**, and **26**) and the target *pf*LDH protein. Compound **4** (8-acetylgoniotriol) formed two conventional hydrogen bonds between the hydrogen atoms on the lactone ring

and linker with the oxygen of Glu122 at distances of 1.73 Å and 1.87 Å. The presence of hydroxyl groups on the linker part of **4** could lead to the formation of conventional hydrogen bond interaction with Tyr85 at a distance of 2.62 Å. The aromatic ring in compound **4** formed π -alkyl interactions with Ile54 (5.00 Å) and Val26 (5.27 Å). Also, the carbon-hydrogen in aromatic ring of **4** formed π -sigma interactions with the π -orbital of Ala98 at a distance of 3.13 Å.

Compound **11** (Parvistone) possesses a hydroxyl group on its linker, which can form a conventional hydrogen bond with Glu122 at a distance of 1.88 Å. The hydrophobic interaction involving chlorine atoms on the linker of compound **11** was observed with the alkyl part of Ile54 (4.81 Å) and Ile119 (4.24 Å). The aromatic ring of compound **11** formed π -alkyl interactions with Ala98 (3.43 Å) and Ile119 (5.33 Å). The π -sigma interaction was observed between the carbon-hydrogen in the aromatic ring of compound **11** and the π -orbital of Ile54 at a distance of 3.97 Å.

Compound **26** (3,5-dimethoxy goniothalamine) possesses methoxy groups on its aromatic ring, contributing to hydrogen bond interactions with specific amino acids. Two conventional hydrogen bonds formed between the methoxy groups and Ile54 at a distance of 3.32 and Gly99 at a distance of 3.03 Å. Carbon-hydrogen bond interaction was observed between the carbon atom of the methoxy group in compound **26** and the oxygen atom of Phe52 at a distance of 3.39 Å. The π -sigma interaction was observed between the carbon-hydrogen in the aromatic ring of compound **26** and π -orbital of Ala98 at a distance of 3.47 Å. Also, the aromatic ring of compound **26** formed π -alkyl interactions with Ile54 (4.40 Å) and Ile119 (4.94 Å).

Table 1. The binding energies (kcal/mol) and interaction residues of all studied ligands and standard drugs in the active site of 1CET.

Compound	Binding energy (Kcal/mol)	Conventional Hydrogen bond interacting residues	Carbon Hydrogen bond interacting residues	Hydrophobic interacting residues	Halogen
1	-5.95	-	-	Ala98, Ile54, Ile119	-
2	-5.53	Glu122, Tyr85	-	Ala98, Ile54	-
3	-5.97	Glu122	-	Ala98, Ile54, Ile119, Phe100	-
4	-6.19	Glu122, Tyr85	-	Ala98, Ile54, Val26	-
5	-5.91	-	-	Ala98, Ile54, Ile119, Lys118, Val26	Lys118
6	-5.93	Gly99	-	Ala98, Ile54, Ile119, Phe100	-
7	-5.56	Tyr85	-	Ala98, Ile54, Ile119, Lys118	-

8	-5.56	-	-	Ile119, Lys118	-
9	-5.64	Tyr85	-	Ala98, Ile54, Ile119, Lys118	Asp53
10	-5.56	Gly99, Tyr85	-	Ala98, Ile54, Ile119, Lys118, Phe52, Val26	-
11	-6.22	Glu122	-	Ala98, Ile54, Ile119	-
12	-6.33	Gly99	-	Ala98, Ile54, Ile119, Phe100, Val26	-
13	-5.97	Tyr85	Glu122, Ile119	Ala98, Ile54, Ile119, Val26	-
14	-5.95	Glu122, Tyr85	-	Ala98, Ile54, Ile119	-
15	-6.74	Gly99	-	Ala98, Ile54, Ile119	-
16	-5.54	-	-	Ala98, Ile54, Ile119	-
17	-5.73	Tyr85	-	Ala98, Ile54, Ile119, Phe100	-
18	-5.18	Gly99	Asp53	Ala98, Ile54, Ile119, Phe100	-
19	-5.68	-	-	Ala98, Ile54, Ile119, Val26	-
20	-6.05	Tyr85	-	Ala98, Ile54, Ile119, Lys118	-
21	-5.93	-	Asp53	Ala98, Ile54, Ile119	Asp53, Phe52, Val26
22	-5.90	-	-	Ala98, Ile54, Ile119	-
23	-5.55	-	-	Ala98, Ile54, Ile119	-
24	-5.93	Tyr85	Leu115	Ala98, Ile54, Ile119, Lys118	-
25	-6.07	Tyr85	Leu115	Ala98, Ile54, Ile119	-
26	-6.29	Gly99, Ile54	Phe52	Ala98, Ile54, Ile119	-
27	-5.79	Tyr85	Leu115	Ala98, Ile54, Ile119, Lys118	-
28	-6.15	Tyr85	Leu115, Glu122	Ala98, Ile54, Ile119, Lys118	-
29	-5.91	Gly99	-	Ala98, Ile54, Ile119	Asp53
30	-5.78	Tyr85	-	Ala98, Ile54, Ile119, Lys118	Leu115
Chloroquine	-6.11	Glu122	Glu122	Ala98, Ile54, Ile119, Tyr85	-
Pyrimethamine	-5.88	Glu122, Phe52, Tyr58	-	Ala98, Ile54, Ile119	-

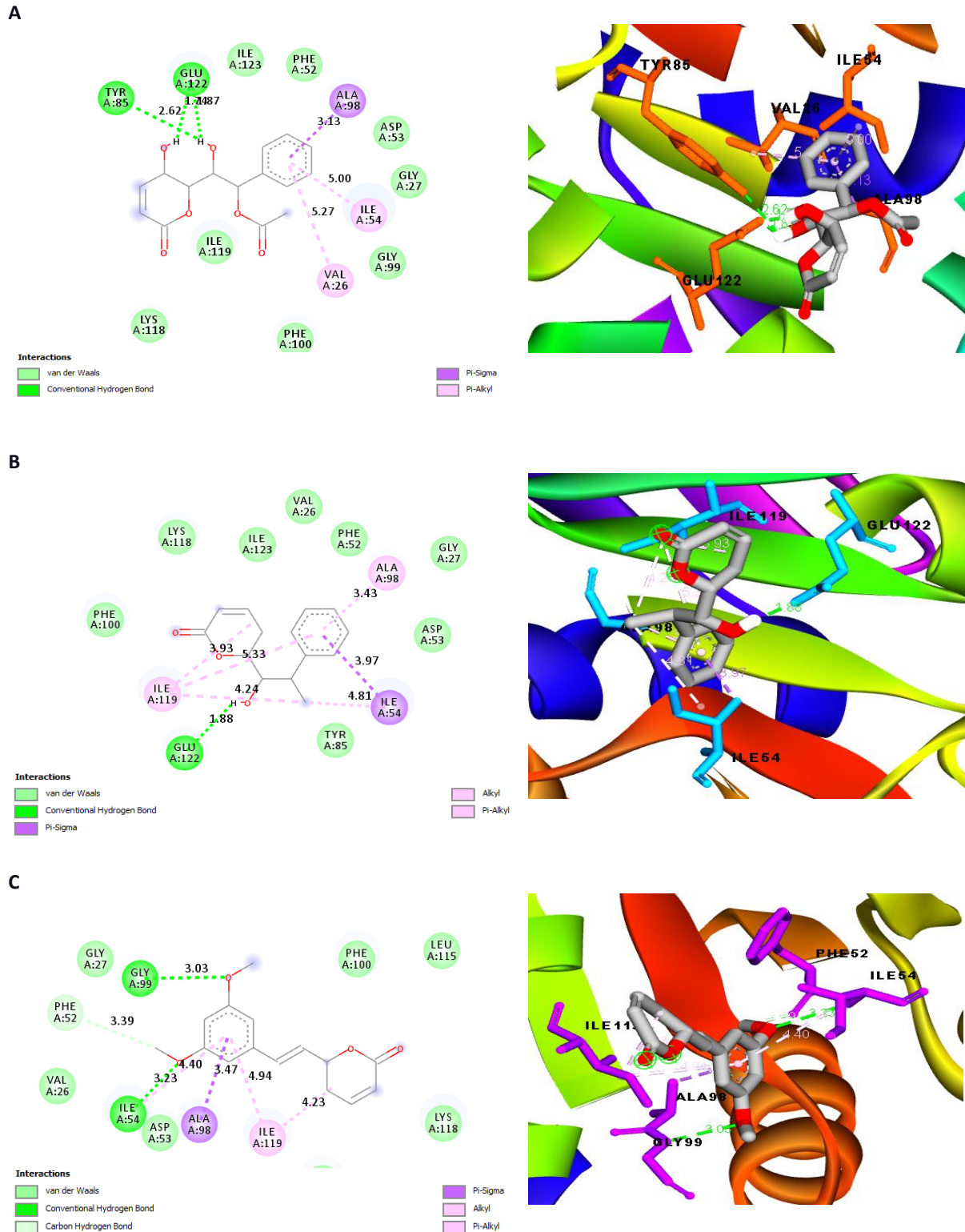


Figure 4: 2D and 3D binding site of A) 8-acetylgoniotriol **4**, B) parvistone **11**, C) 3,5-dimethoxy goniothalamin **26** in the binding pocket of *pf*LDH receptor.

Table 2. Toxicity risks and drug-likeness of the selected compounds.

Compounds	Toxicity risks ^a				Bioavailability and drug score properties ^b			
	MUT	TUM	IRRIT	RE	CLP	S	DL	DS
4	●	●	□ ^e	●	-0.19	-1.86	-2.10	0.42
11	○ ^c	●	○	○	1.80	-2.79	-5.57	0.10
26	●	●	●	●	2.00	-2.97	-12.56	0.45
Pyrimethamine	○	●	○	○	2.54	-4.91	-0.24	0.11
Chloroquine	○ ^c	●	○	●	4.01	-4.06	7.39	0.25

a MUT: mutagenic; TUM: tumorigenic; IRRIT: irritant; RE: reproductive effect.

b CLP: ClogP; S: Solubility; DL: drug likeness; DS: drug score.

c ○: white circle; d ●: black circle; e □: square

Toxicity Properties and Drug-likeness Analysis

Drug-likeness is a measure used to determine a molecule's similarity to existing drugs based on its structural features and molecular properties. Toxicity risk predictors were used to assess potential toxicity risks associated with the compounds. The mutagenicity, tumorigenicity, irritating, and reproductive effects of the compounds were evaluated by bullet code. High-risk properties with undesired effects are shown in the white circle code. A square code indicates a slight risk, and a black circle code indicates drug-conforming behavior. From the data in **Table 2**, compound **26** showed non-mutagenicity, non-tumorigenicity, and non-irritation with no reproductive system toxicity compared with standard drugs. However, Compound **4** exhibited a slight risk of irritants. Compound **11** showed highly mutagenic, irritant, and reproductive, but it conformed to drug-like behavior for tumorigenic. Compounds with logP values less than 5.0 are considered to have a reasonable probability of being well absorbed. All evaluated compounds had logP values below 5.0. Over 80% of marketed drugs have estimated solubility values greater than -4. The solubility of the compounds was found in the range between -1.86 and -2.97. The drug-likeness of the compounds is almost in the comparable zone with that of the standard drug, as shown in **Table 2**. The drug score combines drug-likeness, CLogP, solubility, molecular weight, and toxicity risks in one handy value that can be used to judge the compound's overall potential to qualify for a drug. Compound **26** possesses the highest

drug score, but compound **11** is slightly smaller than the standard drugs.

Physicochemical Properties Analysis

Molinspiration tools were used to analyze the physicochemical of the compound based on Lipinski's Rules of Five (RO5). According to Lipinski's Rules of Five, the compound can serve as a better drug candidate with suitable parameters, including molecular weight ≤ 500 g/mol, $\log P \leq 5$, number of hydrogen bond acceptors ≤ 10 , and number of hydrogen bond donors ≤ 5 . The selected compounds have molecular weight within the acceptable range of ≤ 500 g/mol (**Table 3**). This is important as high molecular weights can impact absorption, diffusion, and transport within the body. The number of hydrogen bond acceptors value of selected compounds is less than 10, and the number of hydrogen bond donors value is less than 5, giving them good solubility in cellular membranes. The result shows all selected compounds obey Lipinski's Rules of Five. All the selected compounds showed lipophilicity (miLogP) values less than 5, which is a positive characteristic of oral availability. The compounds showed less than 140 Å² of topological polar surface area (TPSA), suggesting good solubility. Lower TPSA values suggest better permeability through the blood-brain and gastrointestinal barriers. Other parameters are the number of atoms (natoms), the number of rotatable bonds (nRotb), and molecular volume (volume), all fall within the acceptable ranges, contributing to their conformational flexibility and potential as drug candidates.

Table 3. Physicochemical properties analysis of selected compounds.

Compound	miLogP	TPSA	natoms	MW	nON	nOHNH	nViolations	nRotb	Volume
4	0.91	93.07	21	292.29	6	2	0	5	256.46
11	2.36	46.53	17	252.70	3	1	0	3	217.43
26	3.21	44.77	19	260.29	4	0	0	4	240.72

^a miLogP: logarithm of compound partition coefficient between n-octanol and water; TPSA: topological polar surface area; MW: molecular weight; nON: number of hydrogen bond acceptors; nOHNH: number of hydrogen bond donors; nViolations: number of violations; nRotb: number of rotatable bonds; Volume.

Table 4: Bioactivity scores^a of all the selected compounds.

Compound	GPCRL	ICM	KI	NRL	PI	EI
4	0.14	0.00	-0.39	0.24	0.12	0.46
11	0.20	0.24	-0.04	-0.09	-0.05	0.40
26	-0.01	-0.05	-0.32	0.06	-0.26	0.40

^a GPCRL: GPCR ligand; ICM: ion channel modulator; KI: kinase inhibitor; NRL: nuclear receptor ligand; PI: protease inhibitor; EI: enzyme inhibitor

Table 5: Predicted ADME of all the selected compounds.

Compound	4	11	26
Absorption			
Water solubility (log S)	-2.09	-2.263	-3.671
Caco2 permeability	0.408	1.292	1.345
Human intestinal absorption (% absorbed)	68.102	94.033	97.654
Skin Permeability	-2.873	-2.435	-2.760
P-glycoprotein substrate (yes/no)	No	No	No
Distribution			
VDss (human)	-0.469	0.082	0.030
Fraction unbound (human)	0.322	0.319	0.231
BBB permeability	-0.101	0.232	-0.089
Metabolism			
CYP1A2 (inhibitor) (yes/no)	No	No	Yes
CYP2C19 (inhibitor) (yes/no)	No	No	No
CYP2C9 (inhibitor) (yes/no)	No	No	No
CYP2D6 (inhibitor) (yes/no)	No	No	No
CYP3A4 (inhibitor) (yes/no)	No	No	Yes
Excretion			
Total clearance	0.548	0.338	0.824
Renal OCT2 substrate	No	No	No

Bioactivity Score

The bioactivity of the studied compounds was predicted using molinspiration software, which provides a bioactivity score of the compound against the regular human receptors such as G protein-coupled receptors (GPCR) ligand, ion channel modulator, kinase, nuclear receptor ligand, protease, and enzyme. The bioactivity scores of all studied compounds for drug targets are presented in **Table 4**. Generally, a compound having a high bioactivity score will be active in biological activities. A compound having a bioactivity score of more than 0.00 indicates higher activity, while compounds with values between -0.50 and 0.00 are moderately active, and compounds with values less than -0.50 are inactive. As indicated in **Table 4**, all selected compounds show remarkable biological properties and will produce good physiological actions by interacting with GPCR ligands, ion channel modulators, and other enzymes. The bioactivity score for GPCR ligand activity was between -0.01 and 0.20, suggesting potential activity toward this drug target. The bioactivity scores for ion channel modulator

activity were between -0.05 and 0.24, suggesting their high interaction with this drug target. Bioactivity scores for kinase inhibition modular activity were between -0.39 and -0.04. Bioactivity scores for nuclear receptor ligand and protease inhibitor were observed to be in the range of -0.09 to 0.24 and -0.26 to 0.12, respectively, suggesting potential activity toward these drug targets. The bioactivity score for enzyme inhibitor activity was between 0.40 and 0.46, suggesting potential activity toward this drug target.

ADME Parameters (Pharmacokinetics) Analysis

ADME assessment is crucial in the early stages of drug discovery to identify compounds' potential efficacy and side effects. The ADME parameters of compounds were assessed using Swiss ADME and pkCSM. The results are presented in **Table 5**. A compound is considered to have a high Caco-2 permeability if the predicted value is >0.90 in the pkCSM predictive model. Compounds **11** and **26** were predicted to have high Caco-2 permeability. A compound with less than 30% absorbance indicates low intestinal absorption.

All selected compounds demonstrated high absorption (68.1% to 97.1%). The permeability glycoprotein (P-gp) is important in drug transport, affecting adsorption and disposition. All the selected compounds were found to be non-substrates of glycoprotein. The distribution parameters of the compound were assessed based on the volume of distribution (VDss), fraction unbound, and blood-brain barrier permeability (BBB). The VDss that selected compounds were distributed more in plasma than in tissues. The fraction unbound affects drug efficacy, renal filtration, and hepatic metabolism. The predicted fraction unbound for selected compounds ranged from 0.231 to 0.322. The BBB permeability indicates a drug's ability to cross into the brain. Predicted BBB permeability values ranged from 0.101 to 0.232, suggesting the potential to cross the barrier. Cytochrome P450 (CYP) enzymes are involved in drug oxidative metabolism. Compound **26** was predicted as a potential inhibitor of the CYP1A2 and CYP3A4 enzymes. In the excretion part, the expected total renal clearance was in the medium range of 0.338 to 0.824. All the selected compounds were not found to be substrates for renal uptake transporter in the

proximal convoluted tubule (OCT2).

Molecular Dynamic Simulation

Compound **26** exhibited a lower binding energy score of -6.29 kcal/mol and strongly interacted with important amino acids of *pf*LDH in the docking analysis. Molecular dynamic simulations were conducted to understand the stability of ligand-receptor complexes for the ligand **26** and *pf*LDH protein. The RMSD and The Root Means Square Fluctuation (RMSF) parameters were used to provide information on the stability and relationship of receptor residues in the ligand-protein interaction on the complexes.

Figure 5 displays RMSD plots specifically for ligand **26** throughout the simulation. The RMSD analysis of the ligand provides insights into the conformational stability of the complexes during the simulation course. The RMSD analysis showed ligand **26** remained stable within the protein's binding pocket throughout the simulation. This indicates that the ligand maintained a consistent and stable conformation while bound to the protein.

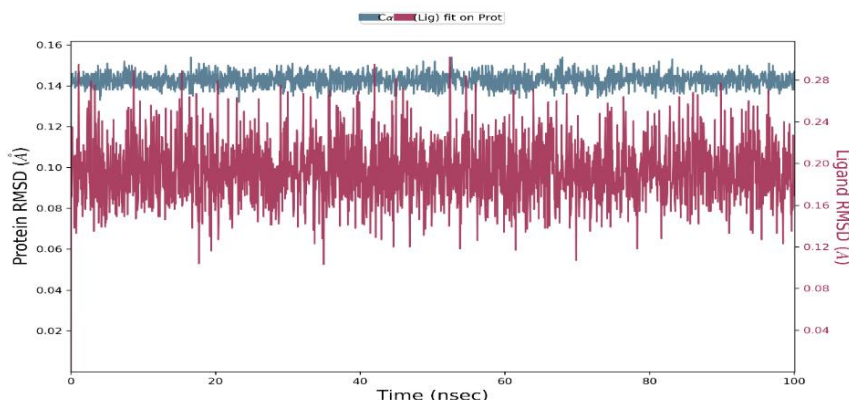


Figure 5. RMSD of ligand **26** with *pf*LDH protein.

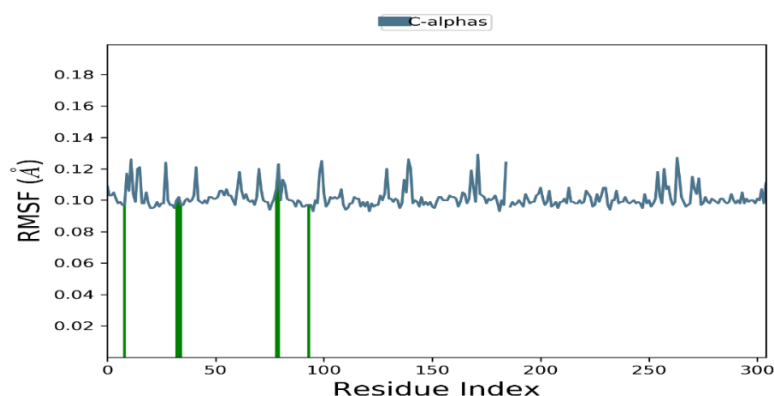


Figure 6. RMSF of ligand **26** with *pf*LDH protein.

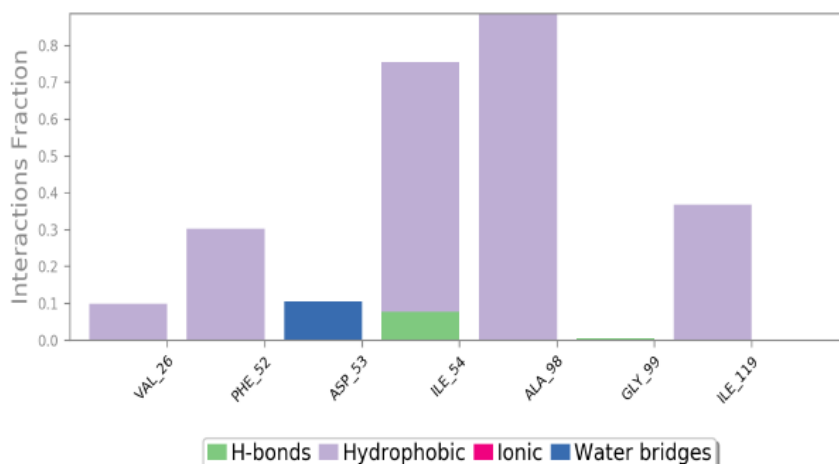


Figure 7. Protein-ligand contacts of ligand **26** with *pf*LDH protein.

RMSF is useful to understand the fluctuations of local changes along the protein chain. **Figure 6** displays the RMSF plot, and peaks indicate areas of the protein that fluctuate the most during the simulation. Noticeably, the tails (*N*- and *C*-terminal) fluctuate more than any other protein part.

Figure 7 shows the protein-ligand interactions of ligand **26** with *pf*LDH protein. The bar chart displayed that hydrogen bonds, hydrophobic, ionic,

and water bridge interaction prevailed during the protein-ligand simulation. Residue Ala98 played a crucial role in forming hydrophobic interactions with compound **26**, and these interactions were maintained effectively at 100 %. The compound and Ile54 also formed hydrophobic interactions, and a small part of hydrogen bonds was clearly observed. The compound and Asp53 formed water bridges. The compound and residues Ile119, Phe52, and Val26 formed hydrophobic interactions that were also clearly observed.

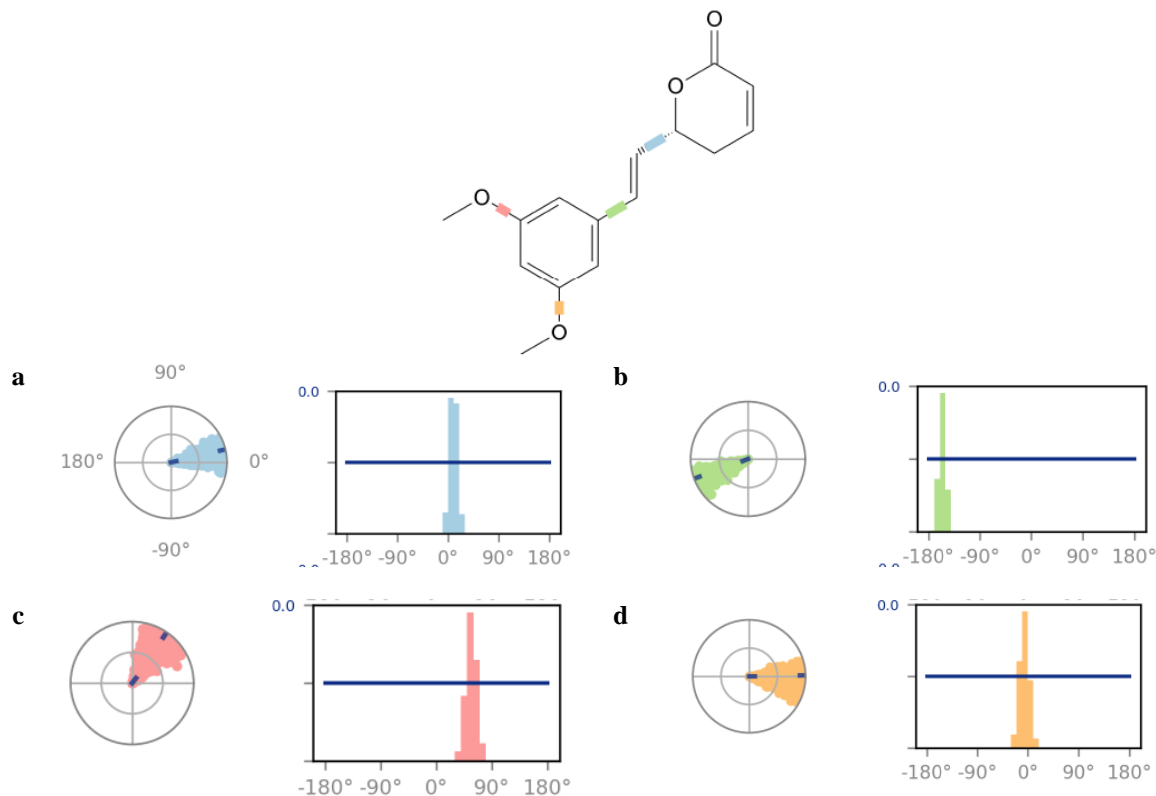


Figure 8. Graphics of the torsional of each rotatable bond of the ligand **26** in the binding pocket of envelope *pf*LDH protein.

The torsional angle for ligand **26** in the binding site of *pf*LDH protein was shown in the combination of **Figure 8**. As depicted in **Figure 8a**, the torsional angle changes promote the π -alkyl interaction between lactone ring and residue Ile119. The torsional angles in bond **b** corresponded to the π -orbital and π -alkyl interactions between the aromatic ring and residue Ala98, Ile54, and Ile119. The torsional angle changes in bond **c** promote the hydrogen bond interaction between the oxygen atom and residue Gly99. Similarly, The torsional angle changes in bond **d** promote the hydrogen bond interaction between the oxygen atom and residue Ile54.

CONCLUSIONS

In conclusion, this study has identified three promising inhibitors of *pf*LDH through molecular docking analysis, compounds **4**, **11**, and **26**. These compounds exhibited better binding energies than the reference drugs chloroquine and pyrimethamine, indicating their potential effectiveness in targeting *pf*LDH. Additionally, they demonstrated interactions with crucial amino acids involved in the chloroquine reaction, further supporting their potential as inhibitors. Moreover, all three compounds passed the Lipinski rule of five and showed promising characteristics in ADME and toxicology analysis, suggesting their suitability as drug candidates. Compound **26** has the highest drug-likeness score, emphasizing its potential as an antimalarial agent. Furthermore, the stability of compound **26** was confirmed over the simulation time, which is a positive indicator of its potential as a drug candidate. However, the *in vitro* or *in vivo* study of the identified compound as a potential antimalarial drug will be necessary to validate the efficacy and safety of these compounds as potential antimalarial drugs.

ACKNOWLEDGEMENTS

The authors would like to acknowledge Universiti Teknologi MARA and Atta-ur-Rahman Institute for Natural Product Discovery (AuRIns) for providing designed labs and facilities for the research. Syahrul Imran would like to thank Universiti Teknologi MARA for the financial support under the Young Talent Researcher (YTR) grant file No. 600-RMC/YTR/5/3 (008/2021).

REFERENCES

1. WHO (2022) *World Malaria Report 2022*. Available at <https://www.who.int/teams/global-malaria-programme/reports/world-malaria-report-2022>.
2. WHO (2018) *World Malaria Report 2018*. Available at <https://www.who.int/teams/global-malaria-programme/reports/world-malaria-report-2018>.
3. Tun, K. M., Imwong, M., Lwin, K. M., Win, A. A., Hlaing, T. M., Hlaing, T. and Woodrow, C. J. (2015) Spread of artemisinin-resistant *Plasmodium*

- falciparum* in Myanmar: A cross-sectional survey of the K13 molecular marker. *The Lancet Infectious Diseases*, **15**(4), 415–421.
4. Plowe, C. V., Kublin, J. G. and Doumbo, O. K. (1998) *P. falciparum* dihydrofolate reductase and dihydropteroate synthase mutations: epidemiology and role in clinical resistance to antifolates. *Drug Resistance Updates*, **1**(6), 389–396.
5. Fidock, D. A., Nomura, T., Talley, A. K., Cooper, R. A., Dzekunov, S. M., Ferdig, M. T. and Wellems, T. E. (2000) Mutations in the *P. falciparum* digestive vacuole transmembrane protein PfCRT and evidence for their role in chloroquine resistance. *Molecular Cell*, **6**(4), 861–871.
6. Syafruddin, D., Josephine, E. S., Sangkot, M. (1999) Mutations in the cytochrome b gene of *Plasmodium berghei* conferring resistance to atovaquone. *Molecular and Biochemical Parasitology*, **104**(2), 185–194.
7. Nishant, J., Rahul, H., Sonal, G., Juveri, K., Jeremy, D., Pawan, K. D. (2022) Highly potent antimalarial activity of benzopyrano(4,3-b)benzopyran derivatives and in silico interaction analysis with putative target *Plasmodium falciparum* lactate dehydrogenase. *Journal of Biomolecular Structure and Dynamics*, **40**(11), 5159–5174.
8. Seoung, R. C., Anupam, P., Nicholas, L. H., Amar, G. C., Babu, L. T., Mitchell, A. (2007) Design, synthesis, and biological evaluation of *Plasmodium falciparum* lactate dehydrogenase inhibitors. *Journal of Medicinal Chemistry*, **50**(16), 3841–3850.
9. Anina, D. M., Naomi, L. U. (1998) Metabolic changes of the malaria parasite during the transition from the human to the mosquito host. *Annual Review of microbiology*, **52**, 561–590.
10. Jon, A. R., Kay, W. W., Rebecca, T., Richard, B. S., R., Leo, B. (1999) Chloroquine binds in the cofactor binding site of *Plasmodium falciparum* lactate dehydrogenase. *Journal of Biological Chemistry*, **274**(15), 10213–10218.
11. Wiart, C. (2007) *Goniothalamus* Species : A Source of Drugs for the Treatment of Cancers and Bacterial Infections ? *Hindawi*, **4**, 299–311.
12. Weber, A., Döhl, K., Sachs, J., Nordschild, A. C. M., Schröder, D., Kulik, A. and Pietruszka, J. (2017) Synthesis and cytotoxic activities of goniothalamins and derivatives. *Bioorganic and Medicinal Chemistry*, **25**(22), 6115–6125.
13. Mohd Ridzuan, M. A., Ruenruetai, U., Noor Rain, A., Khozirah, S. and Zakiah, I. (2006) Antimalarial

- properties of Goniothalamine in combination with chloroquine against *Plasmodium yoelii* and *Plasmodium berghei* growth in mice. *Tropical Biomedicine*, **23**(2), 140–146.
14. Angelo, D. F., Kohn, L. K. and Pilli, R. A. (2006) Cytotoxic activity of (S)-goniothalamine and analogues against human cancer cells. *Biorganic and Medical Chemistry*, **14**, 622–631.
 15. Nafees, A., Sirajudheen, A., Thet, T. H. (2017) Docking based 3D-QSAR Study of tricyclic guanidine analogues of batzelladine K As anti-malarial agents. *Frontiers in Chemistry*, **5**, 1–6.
 16. Favre, A., Carreaux, F., Deligny, M. and Carboni, B. (2008) Stereoselective synthesis of (+)-goniodiol, (+)-goniotriol, (-)-goniofufurone, and (+)-altholactone using a catalytic asymmetric hetero-Diels-Alder/allylboration approach. *European Journal of Organic Chemistry*, **29**, 4900–4907.
 17. Tsubuki, M., Kanai, K., Nagase, H. and Honda, T. (1999) Stereocontrolled syntheses of novel styryl lactones, (+)-goniodiol, (+)-goniotriol, (+)-8-acetylgoniotriol, (+)-goniofufurone, (+)-9-deoxygoniopypyrone, (+)-goniopypyrone, and (+)-altholactone from common intermediates and cytotoxicity of their congener. *Tetrahedron*, **55**(9), 2493–2514.
 18. Dumitrescu, L., Huong, D. T. M., Hung, N. Van, Crousse, B. and Bonnet-Delpon, D. (2010) Synthesis and cytotoxic activity of fluorinated analogues of *Goniothalamus* lactones. Impact of fluorine on oxidative processes. *European Journal of Medicinal Chemistry*, **45**(7), 3213–3218.
 19. Chen, J., You, Z. and Qing, F. (2013) Total synthesis of g-trifluoromethylated analogs of goniothalamine and their derivatives. *Journal of Fluorine Chemistry*, **155**, 143–150.
 20. Ramesh, P., Narasimha, Y., Narendar, T. and Srinivasu, N. (2017) Asymmetry First total synthesis of the highly potent antitumor lactones 8-chlorogoniodiol and parvistone A: Exploiting a bio-inspired late-stage epoxide ring-opening. *Tetrahedron: Asymmetry*, **28**(2), 246–249.
 21. Kasaplar, P., Yilmazar, O. and Cagi, A. (2009) 6-Bicycloaryl substituted (S)- and (R)-5,6-dihydro-2H-pyran-2-ones: Asymmetric synthesis, and anti-proliferative properties. *Biorganic & Medicinal Chemistry*, **17**, 311–318.
 22. De Fatima, A., Modolo, L. V., Conegero, L. S., Pilli, R. A., Ferreira, C. V., Kohn, L. K., De Carvalho, I. E. (2006) Styryl Lactones and Their Derivatives: Biological Activities, Mechanisms of Action and Potential Leads for Drug Design. *Current Medicinal Chemistry*, **13**(28), 3371–3384.
 23. Zhou, F. S., Tang, W. D., Mu, Q., Yang, G. X., Wang, Y., Liang, G. L. and Lou, L. G. (2005) Semisynthesis and Antitumor Activities of New Styryl-Lactone Derivatives. *Chemical & Pharmaceutical Bulletin*, **53**(11), 1387–1391.
 24. De Fatima, A., Luciana, K. K., Joao, E. D. C., Ronaldo, A. P. (2006) Cytotoxic activity of (S)-goniothalamine and analogues against human cancer cells. *Biorganic & Medicinal Chemistry*, **14**, 622–631.
 25. Coura, R., Cezar, J., Caixeta, V., Vendramini-costa, D. B., Ernesto, J., Carvalho, D. and Aloise, R. (2012) Biorganic & Medicinal Chemistry and their in vitro evaluation against human cancer cells. *Biorganic & Medicinal Chemistry*, **20**(11), 3635–3651.
 26. Lipinski, C. A., Dominy, B. W. and Feeney, P. J. (1997) Experimental and computational approaches to estimate solubility and permeability in drug discovery and development settings. *Advanced Drug Delivery Reviews*, **23**, 3–25.
 27. Lipinski, C. A., Lombardo, F., Dominy, B. W. and Feeney, P. J. (2012) Experimental and computational approaches to estimate solubility and permeability in drug discovery and development settings. *Advanced Drug Delivery Reviews*, **64**, 4–17.
 28. Pires, D. E. V., Blundell, T. L. and Ascher, D. B. (2015) pkCSM: Predicting small-molecule pharmacokinetic and toxicity properties using graph-based signatures. *Journal of Medicinal Chemistry*, **58**(9), 4066–4072.
 29. Daina, A., Michielin, O. and Zoete, V. (2017) SwissADME: A free web tool to evaluate pharmacokinetics, drug-likeness and medicinal chemistry friendliness of small molecules. *Scientific Reports*, **7**, 1–13.
 30. Jon, A. R., et al. (1999) Chloroquine binds in the cofactor binding site of *Plasmodium falciparum* lactate dehydrogenase. *Journal of Biological Chemistry*, **274**(15), 10213–10218.
 31. Kenji, O., Kazuhito, S., Hiroshi, H. (2007) Evaluations of molecular docking programs for virtual screening. *Journal of Chemical Information and Modelling*, **47**(4), 1609–1618.
 32. Gregory, L. W., et al. (2006) A critical assessment of docking programs and scoring functions. *Journal of Medicinal Chemistry*, **49**(20), 5912–5931.
 33. Nur, H. Z., Lam, K. W., Nurul, I. H. (2020) Molecular docking study of the interactions between plasmodium falciparum lactate dehydrogenase and 4-aminoquinoline hybrids. *Sains Malaysiana*, **49**(8), 1905–1913.